

Supporting Information

In-situ recycling particulate matter for nanoparticles decorated nitrogen-doped graphene aerogel for high-performance supercapacitor and oxygen evolution reaction

Jiajun Mao^{a,b}, Mingzheng Ge^c, I-Wen Peter Chen^d, Yun Hau Ng^{e,f}, Tianxue Zhu^a, Hui
Liu^c, Jianying Huang^a, Weilong Cai^a, Yuekun Lai^{a*}

^a College of Chemical Engineering, Fuzhou University, Fuzhou 350116, P. R. China

^b Key Laboratory of Bio-inspired Smart Interfacial Science and Technology of
Ministry of Education, School of Chemistry, Beijing Advanced Innovation Center for
Biomedical Engineering, Beihang University, Beijing 100191, P. R. China

^c School of Textile and Clothing, Nantong University, Nantong 226019, P.R. China

^d Department of Applied Science, National Taitung University, Taitung 95092,
Taiwan

^e School of Energy and Environment, City University of Hong Kong, Kowloon, Hong
Kong SAR, P. R. China

^f Particles and Catalysis Research Group, School of Chemical Engineering, University
of New South Wales, Sydney, NSW 2052, Australia

Corresponding Authors E-mail: yklai@fzu.edu.cn

Methods and characterizations: Fabrication of ZIF-67/rGA: In a typical fabricated progress, 15 mL of 4 mg mL⁻¹ GO solution, and 80 mg Co(NO₃)₂·6H₂O was mixed and poured into autoclave. The autolave was put in an electrical oven at 180°C for 10 h. Then result hydrogel was placed in water to remove unreacted ions, and placed in 15 mL dimethyl imidazole (2-MIM) solution (320 mg dimethyl imidazole). Finally, the hydrogels were washed by methanol and water and freeze drying.

Filtration of PM pollution by ZIF-67/rGA: PM capturing by the as-prepared materials was tested in home-built device see our before article. Simply, the materials was put between a smoke environment and a sensitive particle counter (CEM DT-9880M) to form PM@ZIF-67/rGA structure. Filtration efficiency is calculated before and after filtration.

Directly pyrolysis of ZIF-67/rGA: The Co₃O₄/rGA was annealing under nitrogen atmosphere at 500 °C about 30 min, to prevent deformation of the framework. After cooled at room temperature, the sample was transferred into muffle furnace in ambient under 350 °C about 2 h, leading to the conversion of these nanoparticles to cobalt oxide.

Fabrication of nanoporous Co₃O₄/N-rGA: Similarly, the PM@ZIF-67/rGA was annealing under nitrogen atmosphere at 500 °C about 30 min, to prevent deformation of the framework. After cooled at room temperature, the sample was transferred into muffle furnace in ambient under 350 °C about 2 h, leading to the conversion of these nanoparticles to cobalt oxide. Then, the Co₃O₄/N-rGA sample was prepared.

Characterizations: The morphology of aerogels surface were measured by field emission scanning electron microscope (Hitachi S-4800) at 3.0 kV. X-ray photoelectron spectrometer

was employed to evaluate the chemical component via a 100 W Al K α X-ray source. X-ray diffractometer with Cu K α radiation (Philips, X'pert-Pro MRD) was used to characterize the crystal phases of the samples. A transmission electron microscope (FEI Tecnai F-20) was used to survey transmission electron microscopy. N₂ sorption isotherms were measured at a surface area and porosity analyser (ASAP-2020).

Electrochemical measurements: All electrochemical detections were carried at ambient temperature via a three-electrode system at an Autolab electrochemical workstation. The supercapacitor electrodes were fabricated by dispersive active materials (80%), poly(vinylidene difluoride) (10%) and carbon black in ethanol solvent and dried at 60°C for 12 h. Pt and SCE electrodes were used as the counter electrode and reference electrode, respectively. CV, GCD, and EIS on the standard three-electrode system in a KOH solution (6 M) were tested. About the OER performance, glassy carbon (GC) electrodes (3 mm of diameter) were employed in the working electrode. The solution containing catalyst was fabricated via decentralizing 5 mg of active material in 0.55 mL of solution including 500 μ L of isopropanol and 50 μ L of 0.5 wt.% nafion solution and next by ultrasonication for 40 min. Then 4 μ L of the aforementioned suspension was dropped on the GC electrode and dried at ambient temperature. Potentials were transferred to a reversible hydrogen electrode (RHE): $E_{\text{RHE}} = E_{\text{sce}} + 0.242 + 0.059 \times \text{pH}$. All overpotentials (η) were determined on the basis of the following formula: $\eta = E_{\text{RHE}} - 1.23 \text{ V}$. Linear sweep voltammetry was measured under a scan rate of 5 mV s⁻¹ in 0.1 M KOH solution to obtain the polarization curves. All LSV data shown were corrected for iR loss.

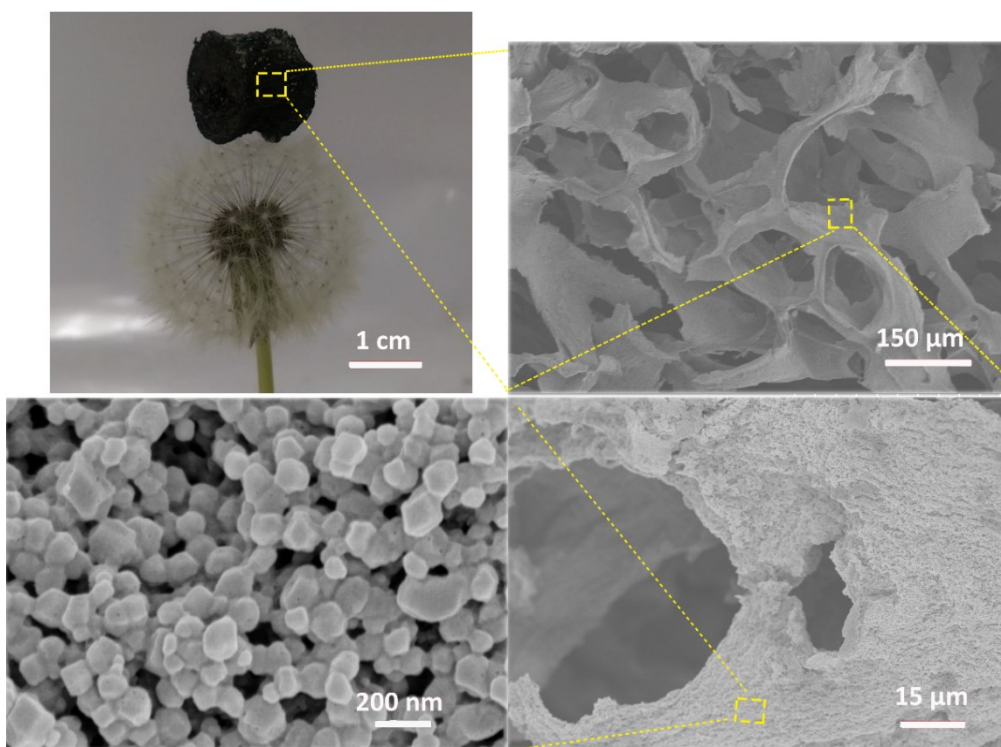


Figure S1. Photography and corresponding SEM images with diverse magnification of as-prepared ZIF-67/rGA.

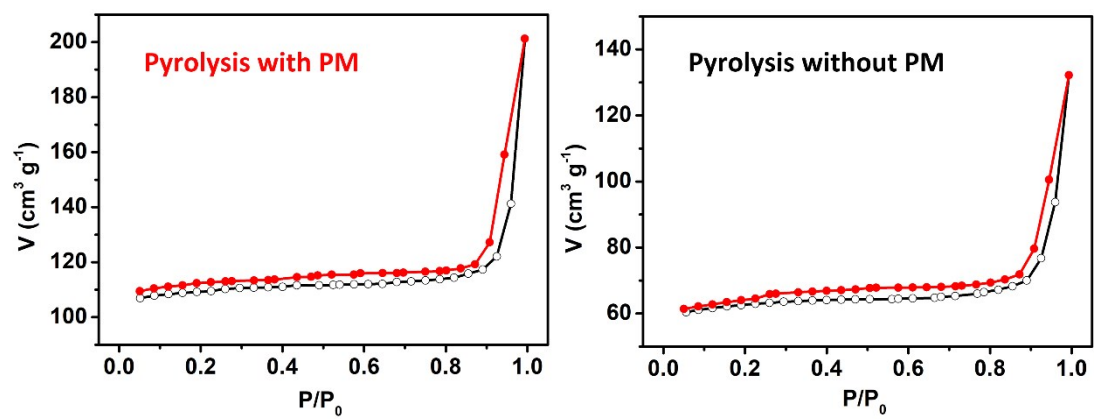


Figure S2. Nitrogen sorption isotherms of pyrolysis of ZIF-67 with PM and without PM.

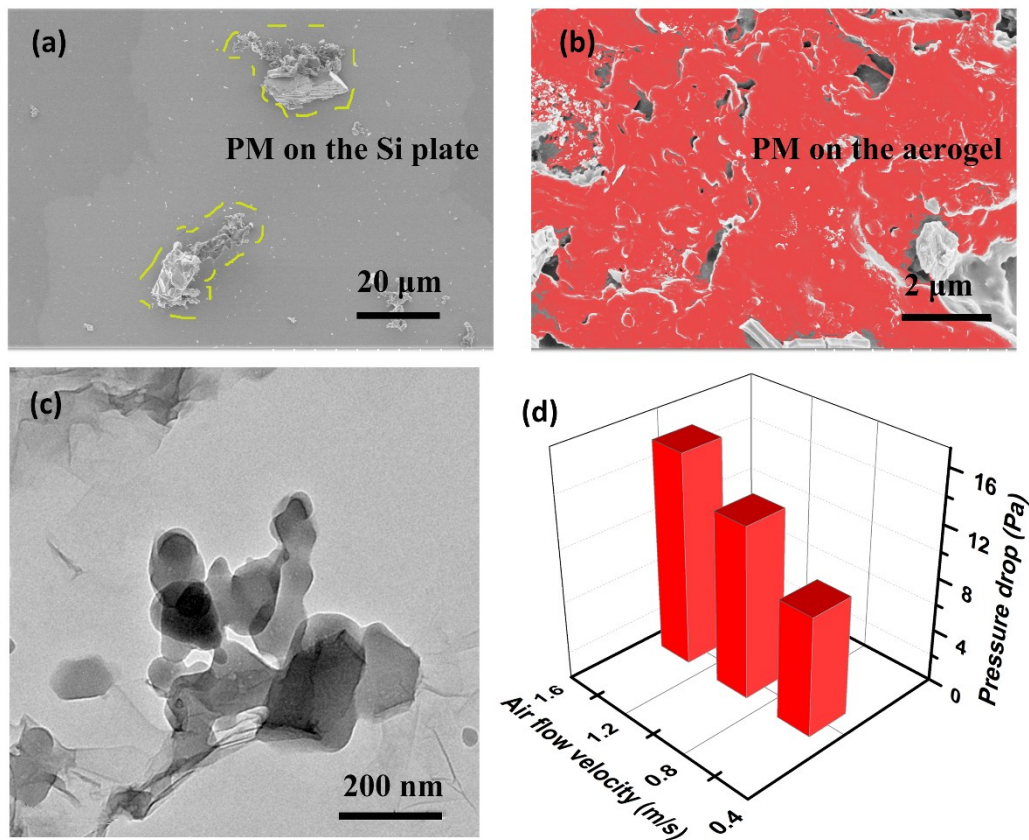


Figure S3. (a) SEM image of PM particle on the silicon plate. Dust particles were accumulated on Si plates (Yellow region). (b) and (c) SEM and TEM pictures of PM adsorbed on the ZIF-67/rGA. (d) Pressure drop of ZIF-67/rGA with 4 mm thickness under diverse air flow velocity.

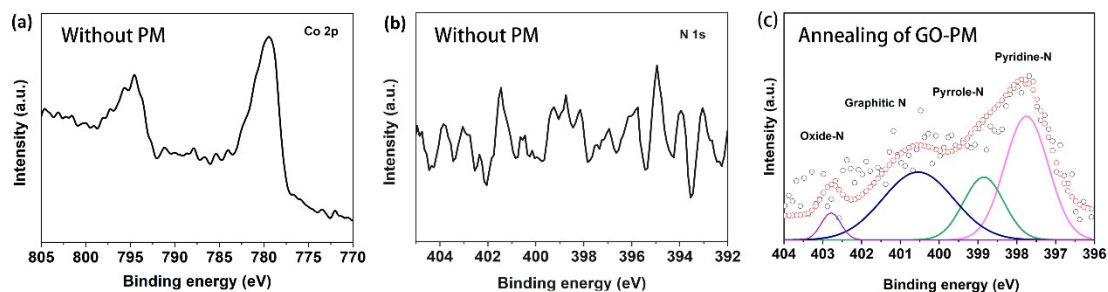


Figure S4. High-resolution (a) Co2p and (b) N1s spectra of the ZIF-67/rGA prepared after thermal annealing.

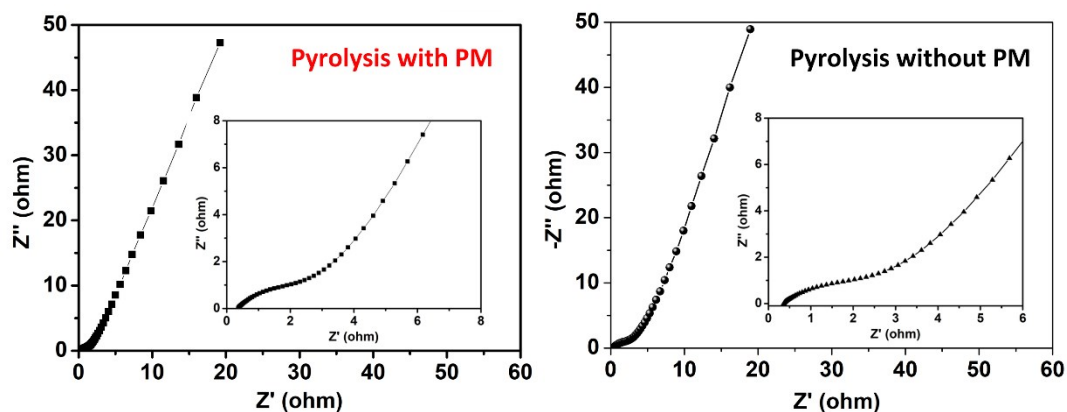


Figure S5. EIS (Nyquist plot) of $\text{Co}_3\text{O}_4/\text{rGA}$ pyrolysis with and without PM electrode in the frequency range of $0.1\text{-}10^5$ Hz.

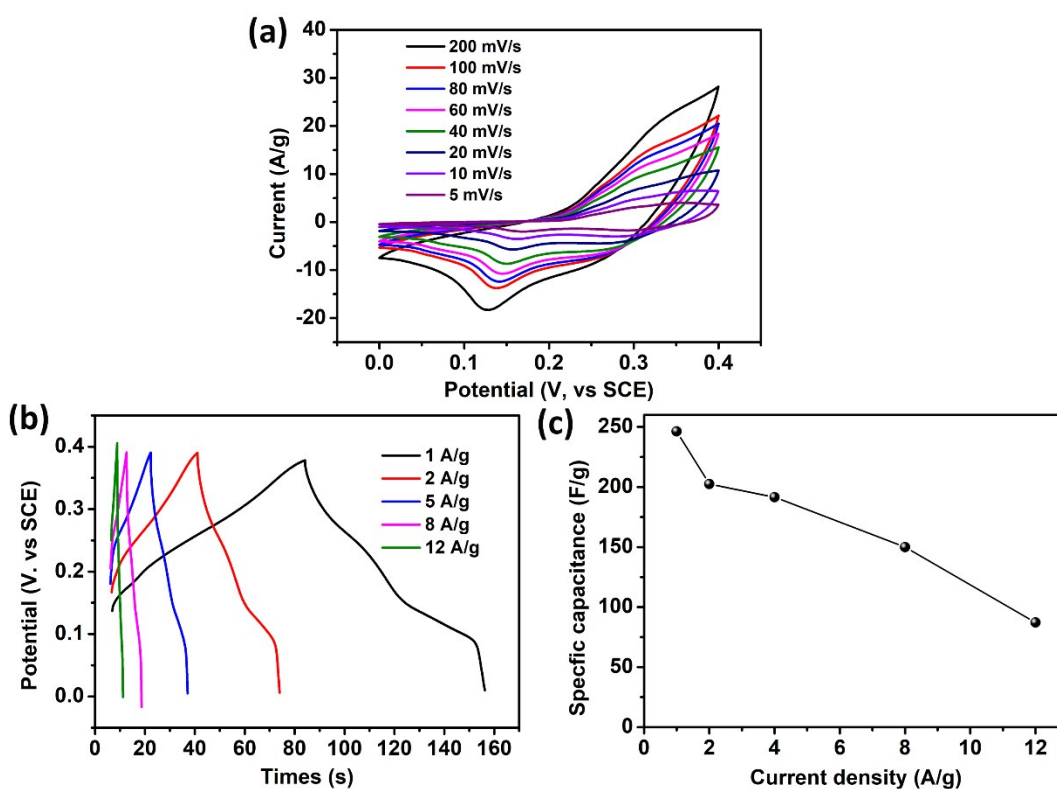


Figure S6. (a) CV of $\text{Co}_3\text{O}_4/\text{rGA}$ electrode without PM at diverse scan rates. (b) Charge-discharge curves of as-prepared electrode at different current intensities. (c) Specific capacitances of the electrode at various current density.

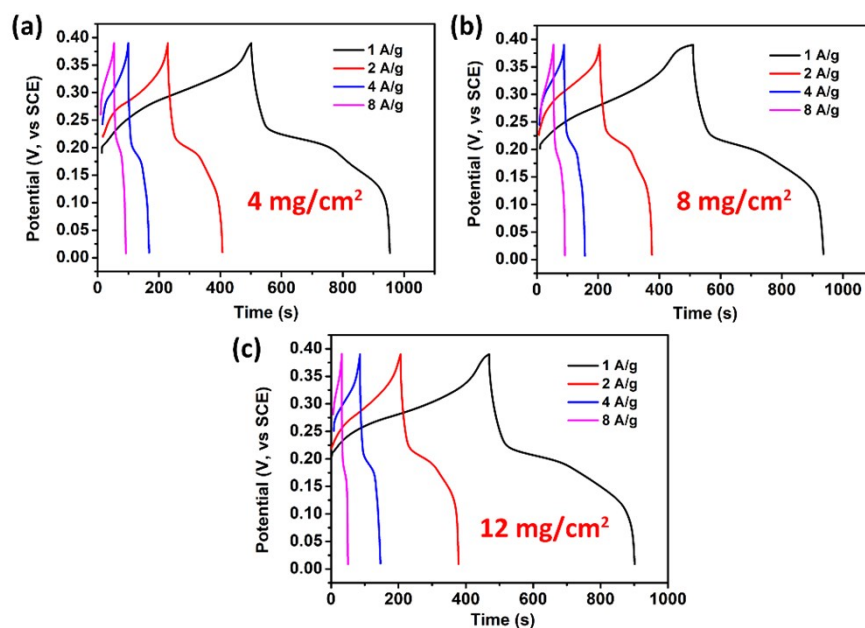


Figure S7. GCD curves of nanoporous $\text{Co}_3\text{O}_4/\text{N-rGA}$ at diverse various intensities for the mass loadings of 4, 8, and 12 mg cm^{-2} .

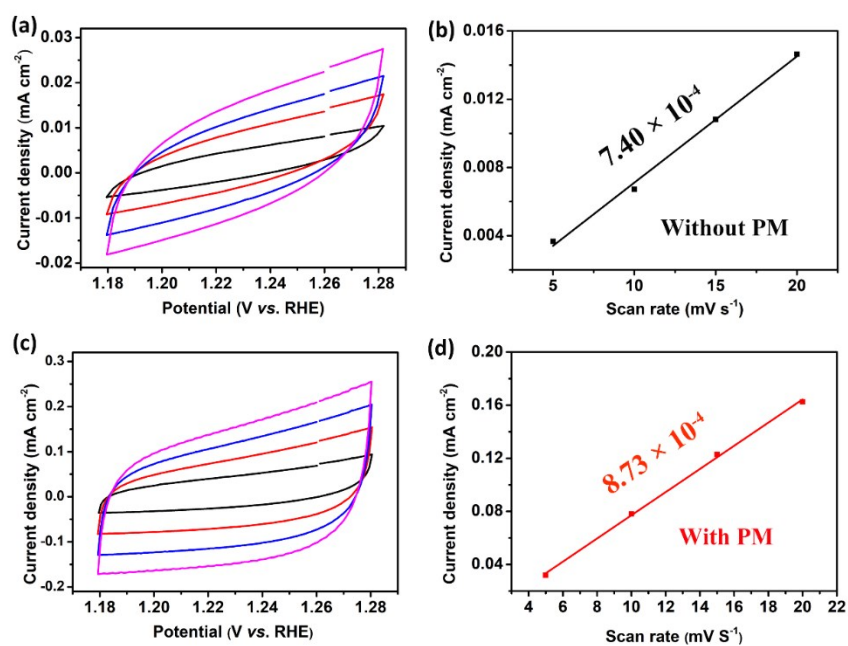


Figure S8. CV curves of (a) $\text{Co}_3\text{O}_4/\text{rGA}$, (c) nanoporous $\text{Co}_3\text{O}_4/\text{N-rGA}$ modified electrodes in the double layer region at scan rates of 5, 10, 15 and 20 mV s^{-1} in 0.1 M KOH solution, and (b), (d) current density as a function of scan rate derived from (a) and (c), respectively.